

Copper Ferrite Revisited

XIAO-XIA TANG, A. MANTHIRAM, AND J. B. GOODENOUGH

Center for Materials Science and Engineering, ETC 5.160, University of Texas at Austin, Austin, Texas 78712

Received November 14, 1988; in revised form January 5, 1989

Reinvestigation of the Jahn–Teller distortion of the copper ferros spinel has established that the critical number of octahedral-site Cu^{2+} ions per formula unit for a cooperative distortion to tetragonal symmetry at room temperature is ca 0.8. Several anomalies associated with the tetragonal–cubic transition have been noted in the literature; these anomalies are shown to reflect not only a tendency for segregation into Cu-rich and Cu-poor regions in the neighborhood of T_t , but also a quenching in of both tetrahedral-site Cu^{2+} and oxygen vacancies on rapid cooling. The intersite exchange $\text{Cu}_A^{2+} + \text{Fe}_B^{3+} = \text{Cu}_B^{2+} + \text{Fe}_A^{3+}$ to reestablish equilibrium becomes facile near 250°C; reoxidation becomes facile near 325°C. This temperature resolution of the two processes in quenched samples is reflected in the temperature variation of the c/a ratio and the electrical resistance below T_t ; these variations can be interpreted in terms of variations in the octahedral-site Cu^{2+} concentration and the associated splitting of the Fe_B^{3+} and Cu_B^{2+} energies. © 1989 Academic Press, Inc.

Introduction

The copper ferros spinel $\text{Cu}_{1-\eta}\text{Fe}_{2+\eta}\text{O}_4$ ($\eta \approx 0.04$), originally believed to have the nominal composition CuFe_2O_4 , is tetragonal at room temperature if annealed in air below 760°C before cooling (1, 2). At equilibrium in air, a tetragonal–cubic transition occurs at $T_t \approx 400^\circ\text{C}$; but as normally prepared by ceramic techniques, a lower T_t is found. For example, associated anomalies in the temperature dependence of the magnetization (3), the permeability (4), and the specific heat (5) have all been reported near 360°C.

Recognition (6–8) that the tetragonal distortion is due to a cooperative Jahn–Teller distortion that is driven by the octahedral-site Cu^{2+} ions has led to a number of experimental and theoretical investigations of this

phenomenon. In copper ferros spinel, four factors complicate the problem.

(i) As recognized early by Néel (9), copper ferrite is a “mixed” spinel containing Cu on both tetrahedral (A) and octahedral (B) sites of the structure, so the distribution of Cu atoms between A and B sites is temperature-dependent. Moreover, non-equilibrium Cu-atom distributions can be quenched in at room temperature. Pauthenet and Bochirol (10) applied this idea to nominal CuFe_2O_4 in an attempt to account for the dependence of the magnetic anomaly, first observed by Takei (3), on the sample history.

(ii) The T_t for a cooperative Jahn–Teller distortion drops off rapidly with decreasing concentration of Jahn–Teller ions as a critical concentration for cooperativity is ap-

proached. Studies made on cooperative Jahn–Teller distortions in spinels containing *B*-site Mn^{3+} ions have established a critical number of *B*-site Mn^{3+} ions per formula unit that varies with different counter cations from 0.9 to 1.3 (11). Moreover, it has also been shown that in the neighborhood of the critical concentration, a local segregation into Mn-rich and Mn-poor regions can be induced by annealing just above T_i (12).

(iii) Stoichiometric $CuFe_2O_4$ cannot be made by conventional high-temperature techniques; it always contains CuO as a second phase (13, 14). As normally prepared, the maximum copper concentration in the spinel system $Cu_{1-\eta}Fe_{2+\eta}O_4$ corresponds to $\eta \approx 0.04 \pm 0.01$ (15).

(iv) The oxygen content of copper ferrosipinel varies with the partial pressure of oxygen and the temperature (16–18). If the oxygen deficiency is present as oxygen vacancies, then the general chemical formula for copper ferrosipinel becomes



where the cations in brackets are in octahedral (*B*) sites and $0.03 \leq \eta \leq 0.5$. In this paper we have chosen an $\eta \approx 0.06$ to ensure a single-phase spinel near the limit of maximum copper concentration.

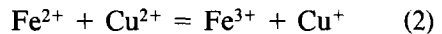
Theoretical work on the variation of x with temperature (9, 19, 20) prompted Ohnishi and Teranishi (21) to investigate the variation of T_i with T_q , where T_i was obtained on samples heated from room temperature after being quenched from an air-anneal temperature T_q . For $T_q \leq 720^\circ C$, their samples were tetragonal at room temperature, but T_i decreased with increasing T_q . A nominal $CuFe_2O_4$ with $T_q = 805^\circ C$ was cubic at room temperature. The cubic sample was heated in air to different intermediate temperatures $T_i < T_q$, then quenched from T_i to room temperature to see at what T_i the compound became tetrag-

onal at room temperature. An anneal at $T_i = 450^\circ C$ for only 5 min transformed the room-temperature structure to tetragonal symmetry whereas the structure remained cubic after 80 hr at $T_i = 320^\circ C$. From these experiments and the earlier observations of anomalous behavior near $360^\circ C$, the authors concluded that a Cu/Fe interchange between *A* and *B* sites becomes facile above $360^\circ C$. No consideration was given to the parameters η and δ , which were assumed to be zero everywhere.

A similar model was used by Stierstadt *et al.* (22) to account for the variation in magnetic properties with x in nominal $CuFe_2O_4$. However, they noted that the x dependence of the Curie temperature T_c was 25 times larger than that calculated from Néel's model of ferrimagnetism. They also showed "aftereffect" evidence for cation intersite migration down to $200^\circ C$.

Brabers and Klerk (15) subsequently reported a lower limit of $\eta \approx 0.04$ for samples prepared at ca. $900^\circ C$; they claimed an $\eta > 0$ supported the suggestion of Ohbayashi and Iida (18) that the changes with temperature in the cation-distribution parameter x , and hence in $T_i(x)$, are due to changes in the oxygen parameter δ , which increases with increasing temperature. This suggestion was based on two observations:

(i) Equilibrium for the reaction



is biased strongly to the right-hand side.

(ii) The Cu^+ ion has a definite tetrahedral-site preference.

Brabers and Klerk also investigated the thermal expansion of sintered samples of $Cu_{0.96}Fe_{2.04}O_{4-\delta}$ quenched from several air-anneal temperatures T_q . Their samples were tetragonal at room temperature if quenched from $T_q \leq 800^\circ C$. Measurements were made in air at $2^\circ C/min$. Anomalous responses signaled the presence of three transition temperatures; they were assigned

to a T'_i associated with the nonequilibrium value of x obtained by quenching, a $T_{ex} > T'_i$ at which the equilibrium value of x is reestablished by a Cu/Fe intersite exchange so that the sample returns to tetragonal symmetry, and a $T_i \approx 400^\circ\text{C}$ corresponding to the tetragonal-cubic transition temperature for the equilibrium value of $x = x(T)$ in air. For this experiment, they assumed that below 400°C any oxygen mobility would be too low in sintered samples for δ to change significantly on the time scale of the anomalous response. The role of variable oxygen parameter with T_q was postulated to change only the Cu/Fe intersite-exchange temperature T_{ex} . They suggested that where a $T_{ex} < T_i$ occurred, there should be a tetragonal-cubic transition at T'_i followed by a cubic-tetragonal transition at T_{ex} and then by a tetragonal-cubic transition at T_i ; T_{ex} appeared to increase with T_q , becoming larger than T_i for $T_q = 800^\circ\text{C}$.

Recently Murthy *et al.* (23) used a two-probe resistivity measurement to monitor the variation of sample resistance with temperature—for heating and cooling cycles in air and argon—on sintered samples of nominal CuFe_2O_4 quenched from different temperatures T_q . Their curves exhibit a complexity and atmosphere dependence that suggest the parameter δ may play a more important role than a simple shifting of T_{ex} .

On the other hand, Nanba and Kobayashi (24) reported a simpler resistivity behavior for a sample with $\eta = 0.104$ that had been quenched from 900°C . For $\eta > 0.1$, the Cu^{2+} -ion concentration turns out to be too low for a static, cooperative Jahn-Teller distortion, which is why the resistivity behavior is simpler. With four-probe resistivity and Seebeck measurements, a constant, positive Seebeck coefficient was found below 250°C . At higher temperatures, the Seebeck coefficient showed important changes with temperature; it became negative above about 290°C and exhibited two cusp-like minima at 360°C and at T_c . Rein-

terpretation of those data is required as the earlier analysis (24) was based on the assumption that Eq. (2) is biased strongly to the left.

Previous experiments have used thermal expansion and resistance as indirect probes of the complex set of transitions occurring in quenched samples. We report a direct measurement of the temperature variation of δ and c/a with temperature for different values of T_q . In addition, differential scanning calorimetry (DSC) is used to provide further information on the processes occurring at the different transition temperatures, including also the ferrimagnetic transition temperature $T_c > T_i$. From furnace-cooled samples of the system $\text{Zn}_\xi\text{Cu}_{0.94-\xi}\text{Fe}_{2.06}\text{O}_4$, the c/a ratio at room temperature is correlated with the B-site Cu^{2+} -ion concentration, which—with a knowledge of δ —allows calculation of the Cu-distribution parameter x at room temperature. Correlation of these measurements with the previously measured thermal expansion (15) and resistance (23) permits four questions to be addressed.

- (i) Is there a $T_{ox} < T_i \approx 400^\circ\text{C}$ where oxidation becomes facile?
- (ii) If so, are T_{ox} and T_{ex} independent of each other?
- (iii) How does T_{ox} and/or T_{ex} change with T_q ?
- (iv) How does the measured resistance track the several transition temperatures?

Experimental

Conventional high-temperature preparations in air of nominal $\text{Zn}_\xi\text{Cu}_{1-\xi}\text{Fe}_2\text{O}_4$ from the constituent oxides all resulted in a small amount of CuO as a second phase. As noted by others for CuFe_2O_4 (13–15), a Cu^+ -ion concentration is stabilized on the tetrahedral sites of the spinel structure at the sintering temperature; any oxidation of the Cu^+ to Cu^{2+} on cooling in air does not

cause an incorporation of the residual CuO into the spinel phase. On the other hand, the high-temperature spinel product indicates that a Cu-deficient spinel is stable, and we were able to prepare single-phase spinels in the system $\text{Zn}_\xi\text{Cu}_{0.94-\xi}\text{Fe}_{2.06}\text{O}_4$ ($0 \leq \xi \leq 0.12$) from stoichiometric mixtures of CuO, Fe_2O_3 , and ZnO. The mixtures were fired in air at 920°C for 1 day, reground, and heated again under the same conditions.

Two types of samples for $\xi = 0$ were prepared for further studies. One group was annealed in air for 1 day at various temperatures $T_q \leq 920^\circ\text{C}$ after slow cooling from 920°C and then quenched into liquid N_2 ; the other was furnace-cooled to room temperature in air from 920°C . The latter are designated 920 N; the former, for example, as 700 Q, where the number refers to the annealing temperature T_q in degrees Celsius.

The absolute oxygen contents of selected samples were determined by weight loss on heating in H_2 at 700°C for 12 hr, a procedure that removes all of the oxygen. The variations in oxygen content with temperature and time on heating/cooling in O_2 and N_2 atmospheres were monitored by TGA with a Perkin-Elmer 7 series thermal analysis system. The same system was also used to obtain the enthalpy changes on heating and cooling in O_2 and N_2 atmospheres by DSC. The DSC measurements were made with about 20 mg of fine powder on an Al pan. In both the TGA and DSC experiments, the base line—measured under identical conditions—was subtracted from the measured values.

Room-temperature X-ray powder-diffraction data were obtained with a Philips diffractometer and $\text{CuK}\alpha$ radiation. High-temperature X-ray measurements were performed with $\text{CuK}\alpha$ radiation and a monochromator on a Rigaku diffractometer; the experiments were carried out in air with a heating rate of $2^\circ\text{C}/\text{min}$ from room temperature to 450°C . While heating the sample, the 2θ range from 40.5 to 45° was scanned cycli-

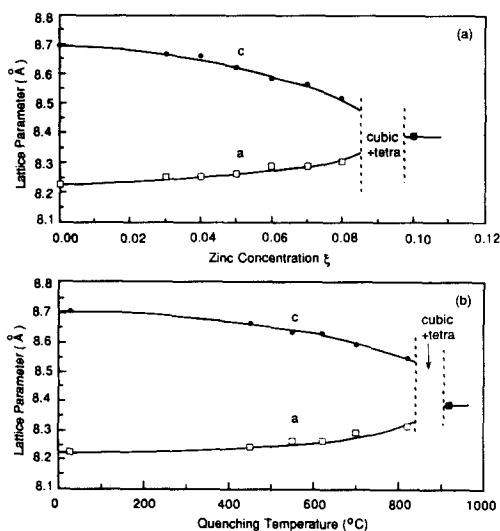


FIG. 1. Variation of c/a ratio (a) with ξ in $\text{Zn}_\xi\text{Cu}_{0.94-\xi}\text{Fe}_{2.06}\text{O}_4$ and (b) with quenching temperature T_q in $\text{Cu}_{0.94}\text{Fe}_{2.06}\text{O}_4$.

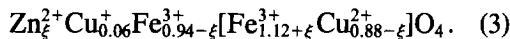
cally at a rate of $2^\circ/\text{min}$ in order to monitor the 400 and 004 reflections, which are particularly sensitive to the tetragonal c/a ratio. The variations of c , a , and hence c/a with temperature were calculated from the positions of these two peaks.

Results and Discussion

The room-temperature lattice-parameter variations with ξ for the system $\text{Zn}_\xi\text{Cu}_{0.94-\xi}\text{Fe}_{2.06}\text{O}_4$ are shown in Fig. 1a. The samples were all furnace-cooled in air, a procedure that, according to absolute oxygen analysis, gives $\delta \approx 0$ in $\text{Cu}_{0.94}\text{Fe}_{2.06}\text{O}_4$. We assume it also does so for all ξ .

The Zn^{2+} ion has a stronger tetrahedral-site preference than Fe^{3+} in the normal spinel $\text{Zn}[\text{Fe}_2]\text{O}_4$; we may assume it also does so in Zn-doped copper ferrite. The Cu^+ ion also has a stronger tetrahedral-site preference than Fe^{3+} , but the Cu^{2+} ion does not. Since the DSC data (see below) shows that furnace cooling in air is slow enough to establish the low-temperature equilibrium distribution of Cu, it followed from Reac-

tion (2) that we may write the chemical formula as



From Fig. 1 we obtain a $\xi_c \approx 0.08$, which corresponds to a critical number $n_c \approx 0.8$ of B -site Cu^{2+} ions per formula unit in this system for a cooperative Jahn–Teller distortion to tetragonal symmetry at room temperature.

The sample with $\xi = 0.09$ was two-phase: cubic and tetragonal. This two-phase region near n_c is due to segregation into Cu-rich and Cu-poor regions because of the stabilization derived by concentrating Jahn–Teller ions in an environment where cooperative elastic coupling—dynamic or static—with other Jahn–Teller ions can occur (12). Indeed, furnace-cooled samples always exhibited a broadening of the reflections strongly dependent on the c -axis whereas quenched samples did not, which rules out inhomogeneities due to insufficient initial mixing of the oxides.

Figure 1b shows the room-temperature lattice parameters of $\text{Cu}_{0.94}\text{Fe}_{2.06}\text{O}_{4-\delta}$ as a function of T_q . The value of δ was obtained from the TGA curves of Fig. 2 and an absolute oxygen analysis after furnace cooling of $\delta \approx 0$. The B -site Cu^{2+} -ion concentration was derived from the c/a ratio with the help of Fig. 1a, which gives c/a vs ξ for furnace-cooled samples in which $\delta \approx 0$ and all the Cu^{2+} ions are on B sites and all the Cu^+ ions are on A sites.

We take the B -site Cu^{2+} -ion population at room temperature to be equal to that in the composition ξ that has the same room-temperature c/a ratio. This procedure is based on two assumptions: (i) the Zn^{2+} concentration is too small to influence appreciably the magnitude of the c/a versus B -site Cu^{2+} -ion concentration and (ii) the tetrahedral-site Cu^{2+} ions do not contribute significantly to the room-temperature c/a ratio, a proposition that is supported by the cubic structure of $\text{Cu}_{0.94}\text{Fe}_{2.06}\text{O}_{4-\delta}$ quenched from

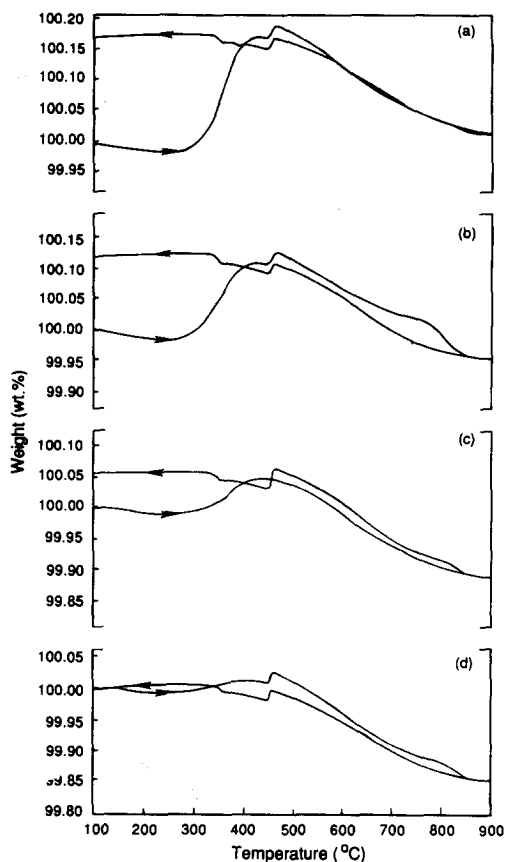


FIG. 2. TGA curves for various $\text{Cu}_{0.94}\text{Fe}_{2.06}\text{O}_4$ samples in O_2 atm: (a) quenched from 920°C , (b) quenched from 700°C , (c) quenched from 550°C , and (d) furnace-cooled.

920°C even though the tetrahedral-site spins are collinear (25). From the Cu^{2+} -ion concentration on B sites and δ , the chemical formula and ionic distribution for each T_q can be derived since the Cu^+ ions can only occupy A sites; this information is summarized in Table I. A room-temperature tetragonal–cubic transition in the range 0.78 to 0.825 B -site Cu^{2+} ions per formula unit is consistent with the critical number $n_c \approx 0.8$ deduced from Fig. 1a and Formula (3).

The TGA curves of Fig. 2 are for heating and cooling in O_2 at $1^\circ\text{C}/\text{min}$. The step in the curves near 480°C marks the ferrimag-

TABLE I
LATTICE PARAMETERS AND CATION DISTRIBUTIONS IN $\text{Cu}_{0.94}\text{Fe}_{2.06}\text{O}_{4-\delta}$

Sample	Lattice parameter (Å)			Oxygen content (4 - δ)	Cation distribution (from c/a ratio, see text)
	a	b	c/a		
920 N	8.229(5)	8.705(2)	1.058	4.00	$\text{Cu}_{0.06}^{1+}\text{Fe}_{0.94}^{3+}[\text{Cu}_{0.88}^{2+}\text{Fe}_{1.12}^{3+}]\text{O}_{4.00}$
550 Q	8.266(5)	8.641(2)	1.045	3.99	$\text{Cu}_{0.08}^{1+}\text{Cu}_{0.025}^{2+}\text{Fe}_{0.895}^{3+}[\text{Cu}_{0.835}^{2+}\text{Fe}_{1.165}^{3+}]\text{O}_{3.99}$
700 Q	8.294(4)	8.598(2)	1.037	3.98	$\text{Cu}_{0.10}^{1+}\text{Cu}_{0.025}^{2+}\text{Fe}_{0.875}^{3+}[\text{Cu}_{0.815}^{2+}\text{Fe}_{1.185}^{3+}]\text{O}_{3.98}$
920 Q	8.392(5)	8.392(5)	1.000	3.97	$\text{Cu}_{0.12}^{1+}\text{Cu}_{0.04}^{2+}\text{Fe}_{0.84}^{3+}[\text{Cu}_{0.78}^{2+}\text{Fe}_{1.22}^{3+}]\text{O}_{3.97}$

netic Curie temperature T_c ; the heating coils introduce a magnetic field at the sample that produces a more important force on the sample below T_c . In the paramagnetic temperature range above $T_c \approx 480^\circ\text{C}$, the weight loss on heating and the weight gain on cooling in air are nearly reversible at a temperature variation of $1^\circ\text{C}/\text{min}$. Since the weight loss on heating is not reversible on cooling in N_2 , we may attribute the weight changes to oxygen loss and reoxidation, respectively, which is the basis of the oxygen analysis reported in Table I. Moreover, all the quenched samples show a weight gain on heating in air beginning above 275°C and reaching a maximum near 400°C . The magnitude of this reoxidation corresponds in all cases to a nearly complete reoxidation to $\delta \approx 0$ calculated from the δ values of Table I.

Figure 2 also shows that, on cooling from 900°C , reoxidation occurs continuously, reaching a saturation value at a second step near 340°C . This second step is caused by the magnetic anomaly at the transition temperature T_t .

In view of the magnetic contribution to the apparent weight below T_c , it is necessary to consider how this contribution might vary with M_s in the quenched vs slow-cooled samples. In order to check the importance of this contribution, the absolute oxygen contents of the quenched and slow-cooled samples at room temperature were determined by weight loss on heating in H_2 at 700°C for 12 hr. The difference in

oxygen content for the two samples corresponded to the weight difference obtained by TGA, which indicates that any effect of magnetism is within experimental error.

These experiments demonstrate two points:

(i) A maximum oxidation state of $\text{O}_{4.0}$ and the retention of chemical homogeneity shows that the oxygen deficiency is accommodated as oxygen vacancies, not cation interstitials.

(ii) Oxygen diffusion is facile above 300°C , which makes $T_{\text{ox}} < T_t$. It appears that the degree of reoxidation varies more significantly with T_q than does T_{ox} itself.

DSC curves for the samples of Table I are shown in Figs. 3–6 for various scanning rates in O_2 and N_2 atmospheres. Figure 3 shows that, on heating, the slow-cooled sample 920 N exhibits two distinct endothermic peaks in both O_2 and N_2 atmospheres. The high-temperature peak near 480°C marks the ferrimagnetic Curie temperature T_c ; it is relatively insensitive to the atmosphere and cycling parameters. Nevertheless, it is lower on cooling after 4 hr in N_2 at 560°C . The lower temperature peak between 350 and 400°C marks the temperature T_t ; it exhibits a pronounced sensitivity on cooling to the atmosphere and time at 560°C . Cycling in O_2 gives a reversible peak at T_t since the oxygen lost on heating is regained on cooling. On the other hand, the oxygen lost in N_2 at 560°C is not regained

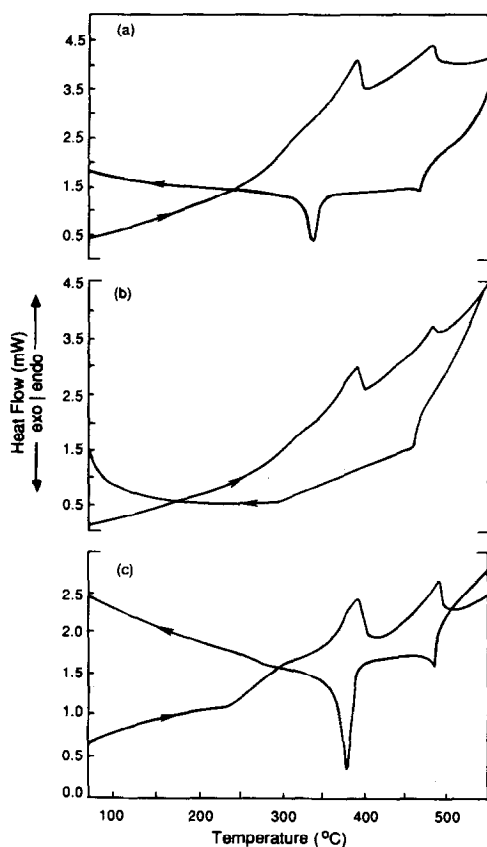


FIG. 3. DSC curves for furnace-cooled, tetragonal $\text{Cu}_{0.94}\text{Fe}_{2.06}\text{O}_4$ (920 N sample) with a heating/cooling rate of $10^\circ\text{C}/\text{min}$ in N_2 atm and staying at 560°C for (a) 1 min and (b) 10 hr, and in O_2 atm and staying at 560°C for (c) 1 min.

on cooling in N_2 . With a 1-min stop at 560°C in N_2 , the amount of oxygen lost lowers T_1 , but is not sufficient to suppress it completely on cooling. After 10 hr at 560°C in N_2 , the tetragonal distortion at room temperature on cooling in N_2 is reduced to $c/a = 1.046$. After 10 hr at 560°C in N_2 , the TGA oxygen loss corresponds to $\delta \approx 0.025$ and hence to ca. 0.83 Cu^{2+} ions per formula unit; if all the Cu^{2+} are on B sites, this number is just greater than $n_c \approx 0.8$.

Figure 7 shows, for comparison, the DSC curves for furnace-cooled $\text{Zn}_\xi\text{Cu}_{0.94-\xi}\text{Fe}_{2.06}\text{O}_{4-\delta}$ samples with $\xi = 0.02$ and 0.04 scanned to 560°C at $10^\circ\text{C}/\text{min}$ in both N_2

and O_2 . As for the $\xi = 0$ sample, the transition at T_1 is reversible in an O_2 atmosphere; but on cooling in a N_2 atmosphere, the transition to the tetragonal phase occurs over a broad temperature range, indicative of a heterogeneous Zn^{2+} -ion distribution; such a heterogeneity is commonly generated in the temperature interval near T_1 if T_1 is high enough for cation mobility. In fact, the sample with $\xi = 0.04$ contained both cubic and tetragonal phases at room temperature. For this sample, a $\delta \approx 0.025$ reduces the number of B -site Cu^{2+} ions to $0.79 \approx n_c$.

The 920 Q sample, which is initially cubic at room temperature, gives the DSC curves of Fig. 4. On heating in N_2 , two endothermic peaks are visible; one near 360°C and a

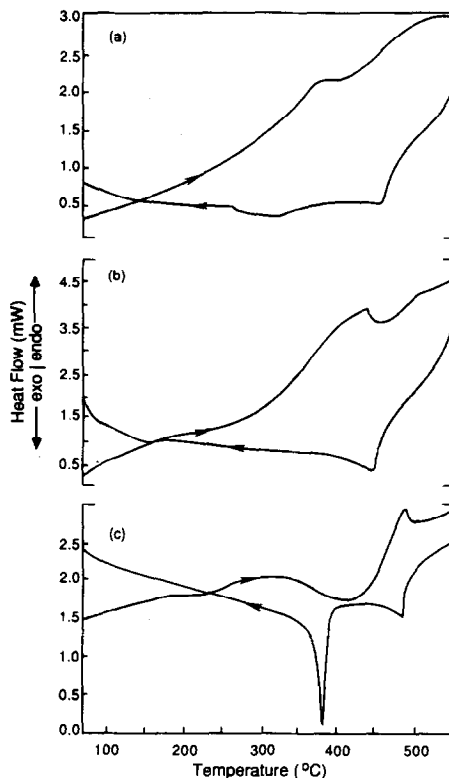


FIG. 4. DSC curves for cubic $\text{Cu}_{0.94}\text{Fe}_{2.06}\text{O}_4$ (920 Q Sample) in N_2 atm with (a) $10^\circ\text{C}/\text{min}$ and (b) $20^\circ\text{C}/\text{min}$, and in O_2 atm with (c) $10^\circ\text{C}/\text{min}$.

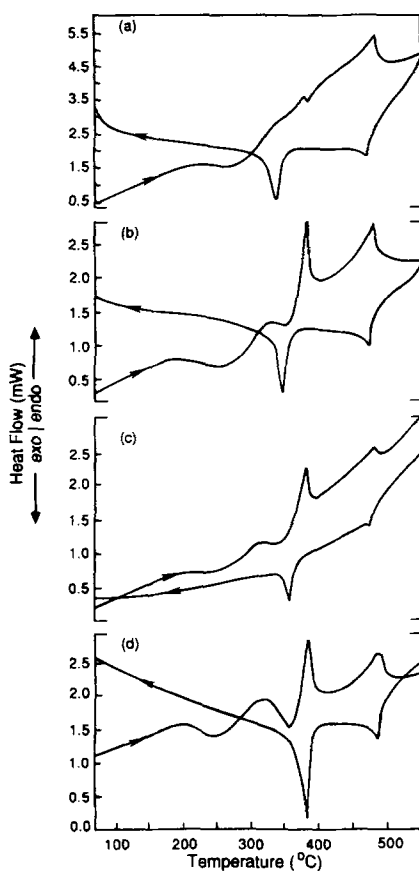


FIG. 5. DSC curves for $\text{Cu}_{0.94}\text{Fe}_{2.06}\text{O}_4$ (550 Q sample) in N_2 atm with (a) $20^\circ\text{C}/\text{min}$, (b) $10^\circ\text{C}/\text{min}$, and (c) $5^\circ\text{C}/\text{min}$, and in O_2 atm with (d) $10^\circ\text{C}/\text{min}$.

broad peak around 520°C . Since the high-temperature X-ray data in air indicate that the 920 Q sample remains cubic on heating to 450°C , the peak near 360° is attributed to a segregation into Cu_B^{2+} -poor and Cu_B^{2+} -rich regions that enhance the cooperative, but dynamic ($n < n_c$) Jahn–Teller stabilization; this introduction of heterogeneity would broaden the peak at T_c . Other factors, such as internal strains induced by quenching, might also contribute to the broadening; but these are expected to be secondary factors. On cooling in N_2 , the peak at T_c is normal, and the peak associated with the cubic–tetragonal transition below 350°C is broad-

ened by the chemical inhomogeneities reintroduced on traversing T_t .

The curves taken in O_2 atmosphere are quite different. In this situation, two broad exothermic peaks are well resolved in the heating curve; one occurs below 250°C and the other is prominent between 350 and 450°C . From the TGA curves of Fig. 2, the prominent exothermic peak above 350°C is due to reoxidation of the sample. From the “aftereffect” evidence for intersite cation exchange down to 200°C cited by Stierstadt *et al.* (22), we may assign the exothermic peak below 250°C to the Cu/Fe intersite exchange reaction

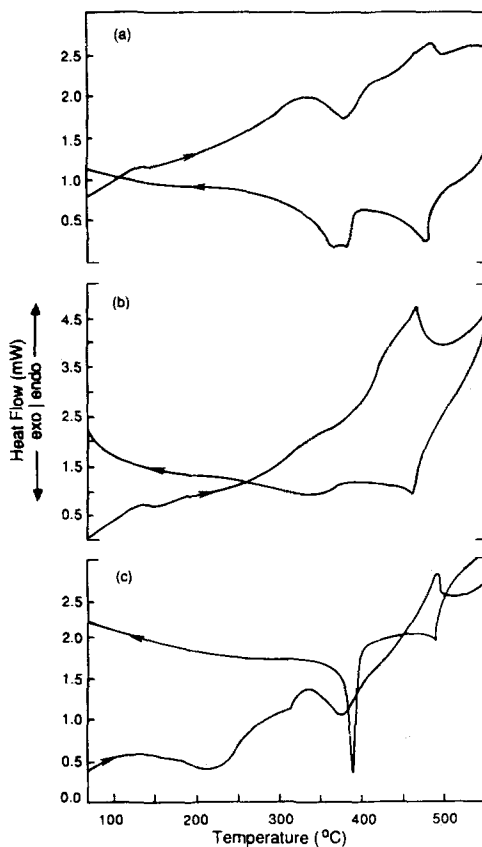


FIG. 6. DSC curves for $\text{Cu}_{0.94}\text{Fe}_{2.06}\text{O}_4$ (700 Q sample) in N_2 atm with (a) $10^\circ\text{C}/\text{min}$ and (b) $20^\circ\text{C}/\text{min}$, and in O_2 atm with (c) $10^\circ\text{C}/\text{min}$.

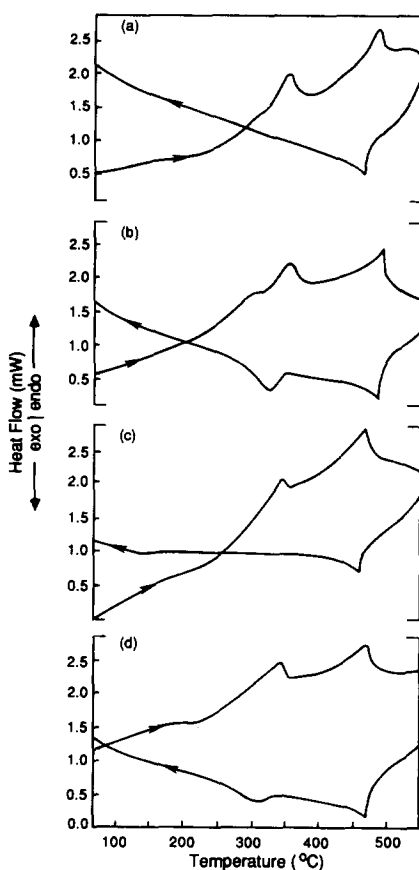


FIG. 7. DSC curves for $\text{Zn}_x\text{Cu}_{0.94-x}\text{Fe}_{2.06}\text{O}_4$ with $10^\circ\text{C}/\text{min}$ (a) $\xi = 0.02$ in N_2 atm, (b) $\xi = 0.02$ in O_2 atm, (c) $\xi = 0.04$ in N_2 atm, and (d) $\xi = 0.04$ in O_2 atm.

From Table I, a significant A-site Cu^{2+} -ion concentration is quenched in at room temperature in the 920 Q sample. Thus we have established the existence of resolvable transition temperatures in the 920 Q sample

$$T_{\text{ex}} < T_{\text{ox}} \approx 400^\circ\text{C} < T_c. \quad (5)$$

With the reestablishing of equilibrium for both the Cu distribution and the oxygen content during the heating cycle in O_2 , the cooling cycle in O_2 exhibits sharp exothermic peaks at both T_c and T_t .

The analogous curves for sample 550 Q (Fig. 5) and sample 700 Q (Fig. 6) are more complex. A cycle rate of $20^\circ\text{C}/\text{min}$ is too

rapid to resolve the various processes and phase transitions that occur, but a rate of $10^\circ\text{C}/\text{min}$ is slow enough, as can be seen by comparison with the $5^\circ\text{C}/\text{min}$ curves.

In addition to the two sharp endothermic peaks marking T_t and T_c , the heating curves of Fig. 5 all show two exothermic peaks: one centered near 250°C marks T_{ex} and one near 350°C marks T_{ox} . (From TGA, it was established that O_2 impurity in the commercial N_2 supply results in a partial reoxidation of the sample on heating even at $10^\circ\text{C}/\text{min}$.) As in the case of the 920 Q sample (Fig. 4), the intersite cation exchange and reoxidation occur at different temperatures and satisfy Eq. (5). On cooling in O_2 , both T_c and T_t remain close to their values on heating; in N_2 both are shifted to lower temperatures, particularly T_t .

The heating curves for the 700 Q sample (Fig. 6) exhibit an endothermic peak at T_c ; the peak marking T_t is shifted from 360°C to below 150°C and is only just visible. The exothermic peak assigned to cation migration is barely visible in N_2 ; it is pronounced in O_2 . The reoxidation exothermic event is also evident above 350°C in O_2 . Between these two exothermic peaks, but overlapping the latter, is an endothermic peak evident in all curves; it marks T_t .

In order to verify by direct means that there is a re-entrant tetragonal phase in the 700 Q sample, it is necessary to monitor the structure as a function of temperature. Figure 8 presents the temperature variations on heating of the lattice-parameter c/a ratios for samples 920 N, 550 Q, and 700 Q in air. Whereas the furnace-cooled sample 920 N exhibits a straightforward variation typical of a first-order transition at T_t , the samples quenched from $T_q = 550$ and 700°C exhibit more complex behavior, sample 700 Q showing the re-entrant tetragonal transition prefigured by the DSC data. Sample 550 Q is particularly interesting; it exhibits a decrease in c/a with increasing temperature that extrapolates to a $T_t < 300^\circ\text{C}$, but the

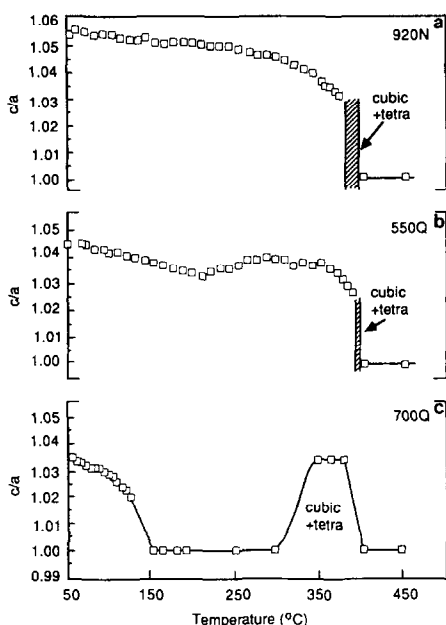


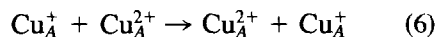
Fig. 8. Variation of c/a ratio with temperature for $\text{Cu}_{0.94}\text{Fe}_{2.06}\text{O}_4$: (a) 920 N sample, (b) 550 Q sample, and (c) 700 Q sample.

intersite cation exchange at T_{ex} increases the c/a ratio in the interval $175 < T < 275^\circ\text{C}$. On further increase of the temperature, the c/a ratio again decreases toward a new $T_t \approx 350^\circ\text{C}$; but in the interval $320 < T < 350^\circ\text{C}$ reoxidation again increases the c/a ratio and increases T_t further to about 380°C . Thus the two processes associated with T_{ex} and T_{ox} are sufficiently resolved to give rise to two separate humps in c/a versus T .

Finally we turn to the resistance data, taken on heating in air, of Murthy *et al.* (23); it is reproduced in Fig. 9. Their curve 510 Q shows a transition from extrinsic to intrinsic conduction above 300°C ; their curve 580 Q shows multiple anomalies in the extrinsic region that qualitatively track the variations in c/a with temperature of our 550 Q sample. Their 900 Q sample exhibits only one large maximum in the region where the DSC curve for our 920 Q sample shows that a large reoxidation occurs; any

anomaly associated with T_{ex} was too small to be evident. From these data, the temperature range where reoxidation impacts the resistance is shifted to higher temperatures as T_q increases.

Interpretation of these data must begin with a model for the extrinsic conduction. In view of Reaction (2) and, according to Table I, the restriction of Cu^+ ions to the A sites, it follows that there are only two important processes to be considered at lower temperatures:



where Reaction (7) is followed by hole conduction on the Fe_B array and electron conduction on the Cu_B array.

The mixed-valent, small-polaron Reac-

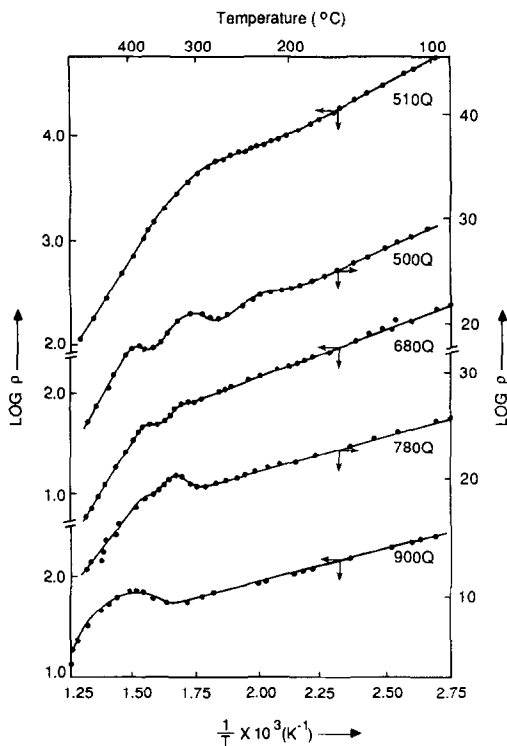


Fig. 9. Variation of electrical resistivity with temperature for nominal CuFe_2O_4 quenched from different temperatures (from Ref. (23)).

tion (6) gives only p -type conduction according to the relative concentrations of Cu^+ and Cu^{2+} ions on A sites in Table I; Seebeck data give n -type conduction for all samples except those quenched from $T_q > 500^\circ\text{C}$ (24). Moreover, the relatively large separation of A -site atoms, especially the A -site Cu atoms, makes it unlikely that Reaction (6) is the dominant mechanism. Finally, Reaction (6) should be sensitive to Cu/Fe intersite exchange, but only for the 580 Q sample in Fig. 9 is there evidence of any sensitivity to this process.

Reaction (7), on the other hand, requires an excitation energy Δ to create mobile carriers on the B sites. The activation energy for the resistivity thus becomes

$$E_A = \frac{1}{2}\Delta + \Delta H_m, \quad (8)$$

where ΔH_m is the motional enthalpy for a charge carrier, electrons on the Cu_B array and holes on the Fe_B array. Whether the net conduction is n -type or p -type depends on the relative magnitudes of the ΔH_m for the electrons and the holes as well as on the relative populations of Cu_B and Fe_B . With this mechanism, it is not difficult to rationalize the change from n -type to p -type conduction with increasing T_q . The change from n -type to p -type conduction on going from annealed, tetragonal samples to quenched, cubic samples has been noted previously (26).

What makes Reaction (7) a plausible alternative for the low-temperature conduction is the small size of the energy Δ separating the donor Fe^{3+} state of the $\text{Fe}^{4+/3+}$ couple and the acceptor Cu^{2+} state of the $\text{Cu}^{2+/+}$ couple. However, with this model we must predict a Δ that increases with the c/a ratio,

$$\Delta = \Delta_0 + \lambda(c/a) + \dots, \quad (9)$$

because the B -site Cu^{2+} ions are stabilized by the cooperative Jahn–Teller distortion. The larger the c/a ratio, the less stable the acceptor $d_{x^2-y^2}$ orbitals at a Cu_B^{2+} ion. Since

the motional enthalpies ΔH_m for the small-polaron motions on the Fe_B and Cu_B arrays should not decrease with c/a , we may anticipate for Reaction (7)

$$E_A = E_0 + \Lambda(c/a) + \dots \quad (10)$$

and indeed Fig. 9 shows a progressive decrease in the measured E_A as T_q is increased, i.e., as c/a is reduced to unity.

Given Reaction (7) as the dominant low-temperature conduction mechanism, comparison of the resistance for the 580 Q sample of Fig. 9 with the variations in c/a ratio for the 550 Q sample of Fig. 8b reveal that, with increasing temperature, the first two humps in the $\log \rho$ versus T^{-1} curves track well the changes in c/a induced first by Cu/Fe intersite exchange and then by reoxidation of the sample. The peak occurring in the interval $350\text{--}400^\circ\text{C}$ marks T_1 ; at this temperature there is a tendency for segregation into Cu-rich and Cu-poor regions, which increases the resistivity.

A remarkable feature of this interpretation of Fig. 9 is the shift to higher temperatures of the re-entrant tetragonal phase with increasing T_q as observed by Brabers and Klerk (15). However, this shift is not the consequence of an increase in T_{ex} as postulated by these authors; rather it appears to be a consequence of the extent of reoxidation required before the concentration of B -site Cu^{2+} ions is high enough to give a cooperative tetragonal distortion above 300°C . In the 900 Q sample of Fig. 9, it would appear that segregation into Cu-rich and Cu-poor regions is being induced in the neighborhood of T_1 , but perhaps without any re-entrant tetragonal phase.

The model presented here allows reinterpretation of the data of Nanba and Kobayashi (24). The exchange Reaction (4) reduces Reaction (6), so the change in sign of the Seebeck coefficient is associated with T_{ex} . The cusp-like minimum at about 360°C reflects T_{ox} ; the filling of oxygen vacancies at T_{ox} increases Δ of Eq. (8)—as does in-

creasing c/a —thereby reducing the concentration of mobile electrons.

Summary

Reinvestigation of the Jahn–Teller distortion of the copper ferros spinel from cubic to tetragonal ($c/a > 1$) symmetry has confirmed the following:

(i) Stabilization of the fully oxidized spinel phase requires some copper deficiency: $\text{Cu}_{1-\eta}\text{Fe}_{2+\eta}\text{O}_4$ with $\eta \approx 0.04$, and the excess iron present as Fe^{3+} introduces η Cu^+ ions per formula unit.

(ii) The transition temperature T_t varies sensitively with the concentration of B -site Cu^{2+} ions; this concentration changes with heat treatment via two factors: (a) excitation of Cu^{2+} ions from B to A sites and (b) loss of oxygen.

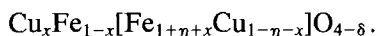
(iii) Metastable oxidation states and Cu-atom distributions may be retained at room temperature by rapid quenching.

(iv) Heating a metastable sample in air may lead to a tetragonal–cubic–tetragonal–cubic phase sequence.

Moreover, the following additional information has been established:

(v) The critical number of B -site Cu^{2+} ions per spinel formula unit for a cooperative Jahn–Teller distortion to tetragonal ($c/a > 1$) symmetry in copper ferros spinel is $n_c \approx 0.8$, which is smaller than that normally found for B -site Mn^{3+} ions in manganospinel.

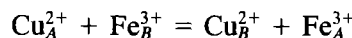
(vi) Any oxygen deficiency is present as oxygen vacancies, not cation interstitials, so we may write the chemical formula as



(vii) In air, the equilibrium value of the oxygen parameter is $\delta \approx 0$ for temperatures $T \leq 350^\circ\text{C}$, and oxidation is facile above 320°C .

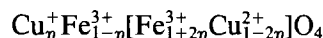
(viii) The intersite cation-exchange reac-

tion



is facile above 200°C .

From (vii) and (viii) it follows that furnace cooling of a copper ferros spinel may give the equilibrium room-temperature chemical formula



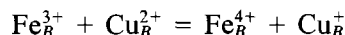
which leads to the prediction, for $n_c \approx 0.8$, of a tetragonal distortion at room temperature for $\eta < 0.1$.

(ix) Heating a metastable sample having $x > \eta$ and $\delta > 0$ at room temperature results in two resolvable temperature domains in which the concentration of B -site Cu^{2+} ions is increased: $200 < T < 275^\circ\text{C}$ via intersite cation exchange and $300 < T < 400^\circ\text{C}$ via reoxidation. This establishes a T_{ox} and

$$T_{\text{ex}} < T_{\text{ox}} < T_t \approx 400^\circ\text{C} < T_c.$$

(x) In the vicinity of T_t , segregation into Cu-rich and Cu-poor domains creates chemical inhomogeneities.

(xi) The dominant conduction process at temperatures $T < T_t$ occurs on the B sites via the reaction



followed by hole conduction on the Fe_B array and electronic conduction on the Cu_B array. The activation energy for this process increases with the axial c/a ratio.

(xii) The degree of reoxidation required to induce a re-entrant tetragonal phase increases with quench temperature T_q . In any dynamic experiment, such as the thermal-expansion measurements of Brabers and Klerk (15), this fact increases the temperature at which a re-entrant tetragonal phase appears; and for $T_q \geq 900^\circ\text{C}$ it may only be manifest as a segregation into Cu-rich and Cu-poor domains. This shift is not due to an increase in T_{ex} with δ as postulated by Brabers and Klerk.

Acknowledgment

The authors thank the Robert A. Welch Foundation of Houston, Texas, for financial support of this research.

References

1. J. L. SNOEK, *Rev. Tech. Philips* **8**, 359 (1946).
2. E. F. BERTAUT, *J. Phys. Radium* **12**, 252 (1951).
3. T. TAKEI, *J. Inst. Elect. Eng. Japan* **59**, 274 (1939).
4. K. STIERSTADT, *Z. Phys.* **146**, 169 (1956).
5. T. INONE AND S. IIDA, *J. Phys. Soc. Japan* **13**, 656 (1958).
6. J. B. GOODENOUGH AND A. L. LOEB, *Phys. Rev.* **98**, 391 (1953).
7. D. S. MCCLURE, *J. Phys. Chem. Solids* **3**, 318 (1957).
8. J. D. DUNITZ AND L. E. ORGEL, *J. Phys. Chem. Solids* **3**, 20 (1957).
9. L. NÉEL, *C. R. Acad. Sci. Paris* **230**, 190 (1950).
10. R. PAUTHENET AND L. BOCHIROL, *J. Phys. Radium* **12**, 249 (1951).
11. J. B. GOODENOUGH, "Magnetism and the Chemical Bond," Interscience and Wiley, New York (1963).
12. J. B. GOODENOUGH, *J. Appl. Phys.* **36**, 2342 (1965).
13. MEXMAIN, *Ann. Chim. (Paris)* **4**, 429 (1969); **6**, 297 (1971).
14. T. YAMAGUCHI, *Proc. Fac. Eng. Keiogijuku Univ.* **19**, 36 (1966).
15. V. A. M. BRABERS AND J. KLERK, *Thermochim. Acta* **18**, 295 (1977).
16. A. BERGSTEIN AND L. CERVINKA, *Czech. J. Phys. B* **11**, 684 (1961).
17. H. M. O'BRYAN, JR., H. J. LEVINSTEIN, AND R. C. SHERWOOD, *J. Appl. Phys.* **37**, 438 (1966).
18. K. OHBAYASHI AND S. IIDA, *J. Phys. Soc. Japan* **23**, 776 (1967).
19. G. I. FINCH, A. P. B. SINHA, AND K. P. SINHA, *Proc. R. Soc. London A* **242**, 28 (1957).
20. P. J. WOCTOWICZ, *Phys. Rev.* **116**, 32 (1960).
21. H. OHNISHI AND T. TERANISHI, *J. Phys. Soc. Japan* **16**, 35 (1958).
22. K. STIERSTADT, H. BENZ, AND H. RECHENBERG, in "Proceedings, Int. Conf. Magnetism, Nottingham," p. 609 (1964).
23. K. S. R. C. MURTHY, S. MAHANTY, AND J. GHOSE, *Mater. Res. Bull.* **22**, 1665 (1987).
24. N. NANBA AND S. KOBAYASHI, *Japan. J. Appl. Phys.* **17**, 1819 (1978).
25. J. B. GOODENOUGH, *Phys. Rev.* **171**, 466 (1968).
26. A. A. GHANI, S. A. MAZEN, AND A. H. ASHOUR, *Phys. Status Solidi A* **84**, 337 (1984).